OBSTACLE AVOIDANCE WITH SIMULTANEOUS TRANSLATIONAL AND ROTATIONAL MOTION CONTROL FOR AUTONOMOUS MOBILE ROBOT

Masaki Takahashi, Takafumi Suzuki, Tetsuya Matsumura and Ayanori Yorozu

Dept. of System Design Engineering, Keio University, 3-14-1 Hiyoshi, Kohoku-ku, Yokohama 223-8522, Japan

Keywords: Service Robot, Obstacle Avoidance, Omni-directional Platform, Fuzzy Potential Method.

Abstract: This paper presents a real-time collision avoidance method with simultaneous control of both translational and rotational motion with consideration of a robot width for an autonomous omni-directional mobile robot. In the method, to take into consideration the robot's size, a wide robot is regarded as a capsule-shaped case not a circle. With the proposed method, the wide robot can decide the direction of translational motion to avoid obstacles safely. In addition, the robot can decide the direction of the rotational motion in real time according to the situation to perform smooth motion. As an example of design method of the proposed method, novel control method based on the fuzzy potential method is proposed. To verify its effectiveness, several simulations and experiments using a real robot are carried out.

1 INTRODUCTION

Various obstacle avoidance methods and their availabilities for mobile robots have described (Du, 2007)-(Dieter, 1997). Most of these studies regard the robots as points or circles and discuss control methods of translational motion. In these studies, a non-circle robot is regarded as a circle robot with consideration of maximum size of the robot. The effectiveness of avoiding obstacles by this approach has been confirmed. However, depending on the shape of the robot, this approach reduces and wastes available free space and can decrease the possibility that the robot reaches the goal. If wide robots, which are horizontally long, are regarded as circles in accordance with conventional approaches, they may not be able to go between two objects due to the largest radius of the robot, even if they ought to be able to go through by using their shortest radius. This suggests the necessity of a suitable orientation angle at the moment of avoidance. Consequently, to enable wide robots to avoid obstacles safely and efficiently, it is necessary to control not only a translational motion but also a rotational motion. In our current research, a wide robot with omni-directional platforms shown in Figure 1 is developed.

Several studies have focused on the orientation

angle of the robot (Kavraki, 1995)(Wang and Chirikjian, 2000). In these studies, by convolving the robot and the obstacle at every orientation and constructing the C-space, the suitable orientation angles of the robot for path planning are decided. However, these methods require an environmental map and the studies have not shown the effectiveness for avoidance of unknown obstacles by autonomous mobile robots. Therefore, to avoid unknown obstacles reactively with consideration of the orientation angle, wide robots need an algorithm that can decide the orientation angle and rotational velocity command in real time based on current obstacle information.

This study proposes a control method of both translational and rotational motion with consideration of a robot width in order to achieve a smooth motion. With the proposed method, the

Figure 1: An autonomous robot for hospital use.

Figure 2: Two robots which are included in respective circles.

Figure 3: Capsule-shaped case.

orientation angle is controlled easily in real time. To verify the effectiveness of the proposed method, several simulations and experiments using our robot shown in Figure 1 are carried out.

2 SIMULTANEOUS TRANSLATIONAL AND ROTATIONAL MOTION CONTROL

2.1 Problem for Solution

There are various non-circle robots. These are vertically long robots, or wide robots. These robots have two arms mounted on a torso with wheels so these robots can be used for mobility, manipulation, whole-body activities, and human-robot interaction (Ambrose, 2004)(Takahashi, 2009). For these wide robots, conventional obstacle avoidance methods are incompatible because they regard the robot as a point or a circle. We are developing a wide robot with a torso, two arms and a head shown in Figure 1. It not only moves indoors but also communicates and interacts with humans through gestures or speech. When the robot opens one or both of its arms slightly, as shown in Figure 2(b), it becomes increasingly difficult to apply conventional obstacle avoidance methods. If these wide robots are regarded as circles in accordance with conventional approaches, it may not be possible for them to go

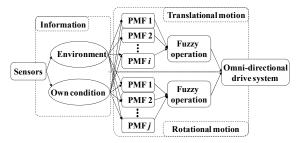between two obstacles due to the largest radius of the robot, even if they

Figure 4: Concept of fuzzy potential method using both translational and rotational motion with an omni-direction platform.

ought to go through by using their shortest radius. In this study, a capsule-shaped case is introduced to make wide robots move smoothly and safely in an environment with obstacles.

2.2 Design of Capsule-shaped Case

The capsule-shaped case is modeled by two circles and two lines tangent to the circles as shown in Figure 3. This closed contour is defined as $l(\phi)$ with the origin at the point P_O.

$$l(\phi) = \begin{cases} & 0 \le \phi < \phi_1 \\ C_a / \cos\phi & if \ \phi_4 \le \phi < 2\pi \\ -C_a / \cos\phi & if \ \phi_2 \le \phi < \phi_3 \\ \sqrt{X(\phi)^2 + Y(\phi)^2} & if \ \begin{matrix} \phi_1 \le \phi < \phi_2 \\ \phi_3 \le \phi < \phi_4 \end{matrix} \end{cases} \quad (1)$$

where ϕ_i is clockwise from the back direction of the robot.

$\phi_1 = \arctan(C_L / C_a)$, $\phi_2 = \pi - \arctan(C_L / C_a)$,
$\phi_3 = \pi + \arctan(C_R / C_a)$, $\phi_4 = 2\pi - \arctan(C_R / C_a)$
$X(\phi)$ and $Y(\phi)$ are calculated as follows.

$$X(\phi) = \begin{cases} \dfrac{-C_L - \sqrt{C_L^2 - (C_L^2 - C_a^2)\{1 + \tan^2(\pi/2 - \phi)\}}}{1 + \tan^2(\pi/2 - \phi)} \\ \quad if \ \ \phi_1 \le \phi < \phi_2 \\ \dfrac{C_R + \sqrt{C_R^2 - (C_R^2 - C_a^2)\{1 + \tan^2(\pi/2 - \phi)\}}}{1 + \tan^2(\pi/2 - \phi)} \\ \quad if \ \ \phi_3 \le \phi < \phi_4 \end{cases} \quad (2)$$

$$Y(\phi) = X(\phi) \tan(\pi/2 - \phi) \quad (3)$$

In the proposed method, C_L, C_R, and C_a are decided in a way that makes wide robot shape fall within the capsule-shaped case.
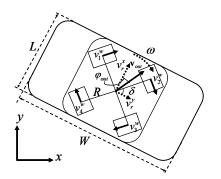
Figure 5: Omni-directional platform with wide body.

2.3 Controller Design

Figure 4 shows a concept of the fuzzy potential method (FPM) that takes into consideration both translational and rotational motion. In the conventional FPM (Tsuzaki, 2003), a command velocity vector that takes into consideration element actions is decided. Element actions are represented as potential membership functions (PMFs), and then they are integrated by means of fuzzy inference. The horizontal axis of PMF is directions which are from $-\pi$ to π radians measured clockwise from the front direction of the robot. The vertical axis of PMF is the grade for the direction. The grade, direction, and configured maximum and minimum speeds, are used to calculate the command velocity vector.

In this research, in addition to conventional approach the PMFs for translational and rotational motion are designed respectively based not only on environmental information but also the robot's condition. Environmental information and the robot's condition are treated separately and divided into a translation problem and a rotational problem. Then the PMFs of each problem are independently integrated using fuzzy inference. Finally, translational and rotational velocity commands, which are calculated by defuzzification of mixed PMFs, are realized by an omni-directional drive system, as shown in Figure 5.

2.4 PMF for Translational Motion

2.4.1 PMF for Obstacles

To enable a wide robot to avoid obstacles safely and efficiently in real time, a concave shaped PMF μ_{oj}^t ($j = 1, 2, \cdots, n$) shown in Figure 7, which takes into consideration the capsule case, is generated. This PMF is specified by depth and width, which are calculated based on the geometrical relation between an obstacle and the robot as shown in Figure 6. By
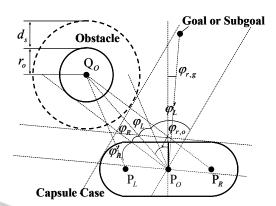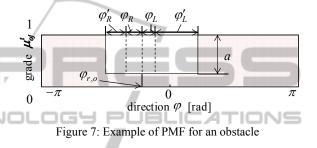

Figure 6: Wide robot and obstacle.

Figure 7: Example of PMF for an obstacle

generating a PMF based on the variables φ_L, φ_R, φ_L', φ_R', a and $\varphi_{r,o}$ in Figure 7, it can choose a safe direction.

$$\varphi_L = \arccos\left(\frac{\left\|\overrightarrow{P_O Q_O}\right\|^2 + \left\|\overrightarrow{P_L Q_O}\right\|^2 - \left\|\overrightarrow{P_O P_L}\right\|^2}{2\left\|\overrightarrow{P_O Q_O}\right\| \cdot \left\|\overrightarrow{P_L Q_O}\right\|} \right). \quad (4)$$

$$\varphi_R = \arccos\left(\frac{\left\|\overrightarrow{P_O Q_O}\right\|^2 + \left\|\overrightarrow{P_R Q_O}\right\|^2 - \left\|\overrightarrow{P_O P_R}\right\|^2}{2\left\|\overrightarrow{P_O Q_O}\right\| \cdot \left\|\overrightarrow{P_R Q_O}\right\|} \right). \quad (5)$$

$$\varphi_L' = \begin{cases} \arcsin\left(D / \left\|\overrightarrow{P_L Q_O}\right\|\right) & \text{if } D < \left\|\overrightarrow{P_L Q_O}\right\|. \\ \pi - \arcsin\left\{\left(\left\|\overrightarrow{P_L Q_O}\right\| - d_s\right) / (D - d_s)\right\} & \text{if } D \geq \left\|\overrightarrow{P_L Q_O}\right\|. \end{cases} \quad (6)$$

$$\varphi_R' = \begin{cases} \arcsin\left(D / \left\|\overrightarrow{P_R Q_O}\right\|\right) & \text{if } D < \left\|\overrightarrow{P_R Q_O}\right\|. \\ \pi - \arcsin\left\{\left(\left\|\overrightarrow{P_R Q_O}\right\| - d_s\right) / (D - d_s)\right\} & \text{if } D \geq \left\|\overrightarrow{P_R Q_O}\right\|. \end{cases} \quad (7)$$

As a measure to decide how far the robot should depart from the obstacle, a is defined as the depth of the concave PMF.

$$a = \frac{\alpha - \left\|\mathbf{r}_{r,o}\right\|}{\alpha - D} \qquad \text{if } \left\|\mathbf{r}_{r,o}\right\| < \alpha . \quad (8)$$

where $\mathbf{r}_{r,o} = (\mathbf{r}_x, \mathbf{r}_y)$ is the current position vector of the obstacle relative to the robot. If the current obstacle position is inside a circle with radius α from the robot position, a PMF for obstacle avoidance is generated. D is decided to ensure a safe distance.

$$D = C_a + r_o + d_s \quad . \tag{9}$$

C_a is the minimum size of the capsule case, r_o and d_s denote respectively the radius of the obstacle and the safe distance. $\varphi_{r,o}$ is the angle of the direction to the obstacle relative to the robot.

$$\varphi_{r,o} = \arctan(\mathbf{r}_y / \mathbf{r}_x) \quad . \tag{10}$$

For safe avoidance, the PMF μ_{oj}^t is generated for all the obstacles that the robot has detected. Then, they are all integrated by calculating the logical product μ_o^t.

$$\mu_o^t = \mu_{o1}^t \wedge \mu_{o2}^t \wedge \cdots \wedge \mu_{oj}^t \quad . \tag{11}$$

By deciding the depth and the base width of the concave PMF μ_o^t is generated.

2.4.2 PMF for a Goal

To head to the goal, a triangular PMF μ_g^t is generated, as shown in Figure 8. μ_g^t is specified by g_a, g_b, and $\varphi_{r,g}$. As a measure to decide how close to the goal the robot should go, g_a is defined as the height of the triangular PMF. As a measure to decide how much the robot can back away from obstacles, g_b is defined. μ_g^t reaches the maximum value as g_a at an angle of the goal direction relative to the front direction of the robot $\varphi_{r,g}$.

$$g_a = \begin{cases} \dfrac{\|\mathbf{r}_{r,g}\|}{\varepsilon} & if \quad \|\mathbf{r}_{r,g}\| \le \varepsilon \\ 1.0 & if \quad \|\mathbf{r}_{r,g}\| > \varepsilon \end{cases} \quad . \tag{12}$$

$$g_b = \eta g_a \quad (0 \le \eta < 1) \quad . \tag{13}$$

where $\|\mathbf{r}_{r,d}\|$ is an absolute value of the position

vector of the goal relative to the robot. ε and η are constants. If $\|\mathbf{r}_{r,d}\|$ is below ε, g_a is defined. The robot can decelerate and stop stably.

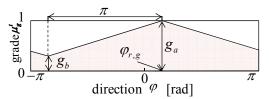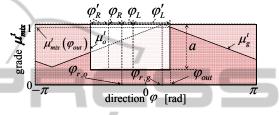Figure 8: Example of PMF for a goal.

Figure 9: Example of mixed PMF for translational motion.

2.4.3 Calculation of a Translational Command Velocity Vector

The proposed method uses fuzzy inference to calculate the command velocity vector. The PMFs μ_o^t and μ_g^t are integrated by fuzzy operation into a mixed PMF μ_{mix}^t as shown in Figure 9. μ_{mix}^t is an algebraic product of μ_o^t and μ_g^t.

$$\mu_{mix}^t = \mu_g^t \wedge \mu_o^t \quad . \tag{14}$$

By defuzzifier, a velocity command vector is calculated as a traveling direction φ_{out} and an absolute value of the reference speed of the robot based on the mixed PMF μ_{mix}^t. φ_{out} is decided as the direction that makes the PMF $\mu_{mix}^t(\varphi)$ maximum.

Based on φ_{out}, v_{out} is calculated as follows.

$$v_{out} = \mu_{mix}^t(\varphi_{out})(v_{max} - v_{min}) + v_{min} \quad . \tag{15}$$

where $\mu_{mix}^t(\varphi_{out})$ is the mixed PMF for translational motion corresponding to the φ_{out}. v_{max} and v_{min} are respectively the upper and lower limits of the robot speed.

2.5 PMF for Rotational Motion

2.5.1 PMF for Obstacles

To enable a wide robot to decide the appropriate angle of the direction for obstacle avoidance in real time, PMF μ_o^r is generated.
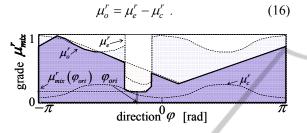
$$\mu_o^r = \mu_e^r - \mu_c^r \; . \tag{16}$$

Figure 10: Example of mixed PMF for rotational motion.

μ_e^r is generated based on the distance from the center of the robot to obstacles corresponding to all directions, as shown in Figure 10. The relative distances are obtained with range sensors such as laser range finder, ultra sonic sensors or infrared sensors. μ_c^r is generated based on the capsule case.

$$\mu_c^r\left(\varphi\right) = \frac{l\left(\varphi + \pi\right)}{\alpha} \; . \tag{17}$$

The aim of the PMF μ_o^r is to search for an orientation angle of the robot that would maximize the distance between a point on capsule case and each obstacle by turning the front or back side of the robot. By using the capsule case, a PMF design can deal with the width of the robot for rotational motion.

2.5.2 PMF for a Goal

In order to turn the front of the robot toward the goal direction or the travelling direction if there is no obstacle to avoid, PMF for a goal is generated as μ_g^r.

This shape is decided in same way as μ_g^t.

2.5.3 Calculation of a Rotational Command Velocity

For the rotational motion, like the translational motion, the rotational command velocity is derived. The PMFs μ_e^r and μ_g^r are integrated by fuzzy operation into a mixed PMF μ_{mix}^r, as shown in Figure 10.

$$\mu_{mix}^r = \mu_g^r \wedge \mu_o^r \; . \tag{18}$$

By defuzzifier, the command velocity is calculated as a rotational direction φ_{ori} and an absolute value of the reference speed of the robot. φ_{ori} is decided as the direction φ_i that makes the following function $h(\varphi)$ minimum.

$$h\left(\varphi\right) = \int_{\varphi - \zeta}^{\varphi + \zeta} \mu_{mix}^r\left(\psi\right) \; d\psi \tag{19}$$

where ζ is the parameter to avoid choosing an uncertainty φ_i caused by, for example, noise on the sensor data. On the basis of φ_{ori}, ω is calculated.

Table 1: Parameters in numerical simulations.

L	0.4 m	W	1.0 m
C_a	0.3 m	C_L	0.3 m
C_R	0.3 m	r_a	0.3 m
d_s	0.3 m	D	0.9 m
α	4.0 m	η	0.2
ε	1.0 m	a_r	1.0 m/s^2
ω_{max}	1.0 rad/s	ω_{min}	0.0 rad/s

$$\omega = \omega_a \, \text{sgn}(\varphi_{ori}) \; . \tag{20}$$

where ω_a is design variable.

2.6 Omni-directional Platform

An omni-directional platform was used for the autonomous mobile robot's motion. The command velocity vector was realized by four DC motors and omni wheels.

$$v_r^x = v_{out} \cos \varphi_{out} \; . \tag{21}$$

$$v_r^y = v_{out} \sin \varphi_{out} \tag{22}$$

where v_{out} and ω are respectively command translational velocity vector and rotational velocity.

$$\begin{bmatrix} v_1^w \\ v_2^w \\ v_3^w \\ v_4^w \end{bmatrix} = \begin{bmatrix} \cos\delta & \sin\delta & R \\ -\cos\delta & \sin\delta & R \\ -\cos\delta & -\sin\delta & R \\ \cos\delta & -\sin\delta & R \end{bmatrix} \begin{bmatrix} v_r^x \\ v_r^y \\ \omega \end{bmatrix} \tag{23}$$

δ is an angle of gradient for each wheel. R is half

the distance between two diagonal wheels. v_i^w is a command velocity of each i-th wheel.

3 SIMULATION RESULTS

To verify the effectiveness of the proposed method, numerical simulations were carried out. In simulations, the robot was presumed to be able to detect obstacles and to have information about the relative position vector. The measuring range was assumed to be 4.0 m in all directions. Each parameter was shown in Table 1.
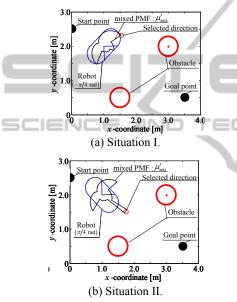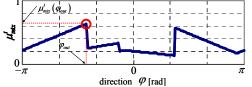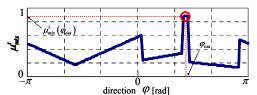

(a) Situation I.

(b) Situation II.

Figure 11: Simulation results.

(a) Situation I: robot cannot find the direction between the two obstacles.

(b) Situation II: robot can find the direction between the two obstacles.

Figure 12: Aspects of mixed PMF for translational motion in two different situations.

3.1 Performance of Capsule Case

To verify the effectivenesses of using capsule case by comparing the results of the chosen direction of robot motion, simulations in two different situations regarding the orientation angle for a wide robot were carried out. In the simulations, the positions of the robot and two obstacles were immobilized at each point respectively $(1.0\,\text{m}, 2.0\,\text{m})$, $(1.5\,\text{m}, 0.5\,\text{m})$ and $(3.0\,\text{m}, 2.0\,\text{m})$, as shown in Figure 11.

Table 2: Position coordinates of start and goal points of the robot and of obstacles.

	Start [m]	Goal [m]	Obstacles [m]				
			1	2	3	4	5
A	(0.0,0.0)	(8.0,0.0)	(2.5,−1.8)	(2.5,−1.2)	(2.5,1.2)	(2.5,1.8)	−
B	(0.0,−2.0)	(11.0,2.0)	(4.0,−2.0)	(4.0,−1.4)	(4.0,1.0)	(4.0,1.6)	(4.0,2.2)
C	(0.0,−2.0)	(11.0,2.0)	(4.0,−2.0)	(4.0,−1.4)	(4.0,0.4)	(4.0,1.0)	(4.0,1.6)

In situation I shown in Figure 11(a), the orientation angle of the robot was fixed to $-\pi/4$ radians clockwise from the x-axis on the absolute coordinates. Therefore the robot faced the goal. Figure 12(a) shows the mixed PMF μ_{mix}^t in this situation. The chosen direction of the robot motion was calculated as -1.35 radians, which was clockwise from the front direction of the robot, as shown in Figure 11(a). As a result, the robot chose a longer route to the goal.

In situation II shown in Figure 11(b), the orientation angle of the robot was fixed to $\pi/4$ radians on the absolute coordinates. In contract to situation I, the robot did not face the goal. Figure 12(b) shows the mixed PMF μ_{mix}^t in this situation. The chosen direction of the robot motion was calculated as 1.37 radians, which was clockwise from the front direction of the robot, as shown in Figure 11(b). As a result, the robot chose a shorter route with no collision.

These two results showed the effectiveness of the capsule case and that the wide robot can decide the direction of translational motion that takes consideration with the robot's orientation, the goal position and the obstacle position simultaneously in real time.

3.2 Obstacle Avoidance

The effectiveness of the proposed method was verified by comparing two design methods based on FPM in three situations. In method I, the wide robot was regarded as a circle with radius 0.6 m. In

method II, the capsule case was used and the width and rotational motion of the robot were taken into consideration. The start and goal positions of the robot and the obstacles are shown in Table 2.

In situation A, the robot with method I did not succeed in going between two objects. It did not collide with the obstacles and did not get to the goal point as shown in Figure 13. On the other hand, in method II, the capsule case and real-time control based on FPM were used. As shown in Figure 14, the robot performed translational and rotational motion simultaneously in real time and succeeded in going between two objects. Figure 15 shows the time history of the orientation angle on the absolute coordinate of the robot. The robot changed the orientation angle according to the situations and succeeded in getting to the goal with the orientation angle 0 radian by using PMF for rotational motion.

In situation B, the robot with method II did not succeeded to going between two objects as shown in Figure 16. The robot found another way and got to the goal point. On the other hand, as shown in Figure 17, the robot with method II performed translational and rotational motion simultaneously in real time.
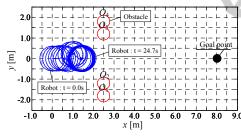

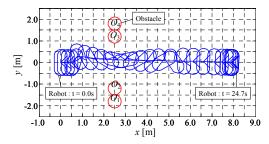Figure 13: Simulation result of method I in situation A.

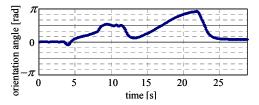Figure 14: Simulation result of method II in situation A.

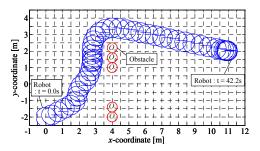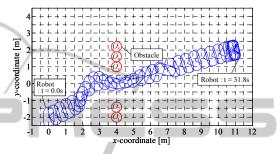Figure 15: Orientation angle of the robot with method II in situation A.

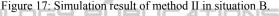Figure 16: Simulation result of method I in situation B.

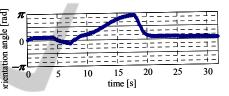Figure 17: Simulation result of method II in situation B.

Figure 18: Orientation angle of the robot with method II in situation B.
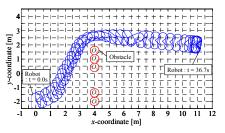

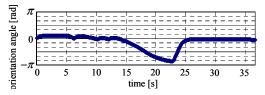Figure 19: A simulation result in the situation C by using method II.

Figure 20: Orientation angle of the robot with method II in situation C.

The time history of the orientation angle on the absolute coordinates of the robot is shown in Figure 18.

11

In situation C, the robot with method II took its own size into consideration using the capsule case and chose a path that did not go between the two obstacles.

These results showed that motion control without a capsule case made it difficult for the robot to go between two objects due to the largest radius of the robot, even if it would be able to go through by using its shortest radius. Applying the capsule case to a wide robot, the robot can decide the orientation angle according to the situation. As a result, the robot can get to the goal point smoothly and safely.
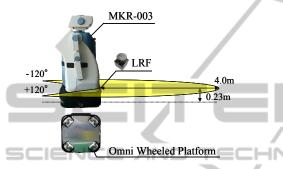

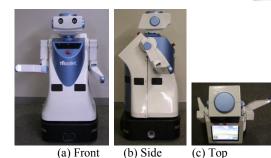Figure 21: Laser sensor and an omni-directional platform on an autonomous mobile robot.

(a) Front   (b) Side   (c) Top

Figure 22: Experimental situation.

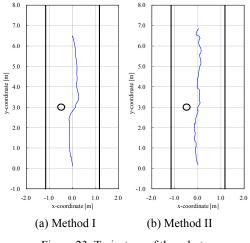

(a) Method I   (b) Method II

Figure 23: Trajectory of the robot.

4 EXPERIMENTAL RESULTS

To verify the performance of the proposed collision avoidance method to static obstacles, an experiment using the real robot were carried out. In order to recognize the environment, as shown in Figure 21, the robot has external sensors, such as a stereo camera, laser range finder and ultrasonic sensors. However, in this research the robot recognizes the environment using only laser range finder.
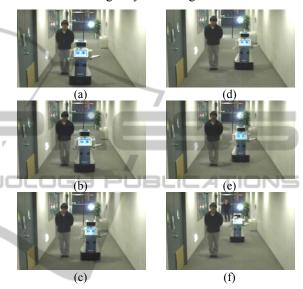

(a)   (d)

(b)   (e)

(c)   (f)

Figure 24: Experimental result to static human using fuzzy potential method without PMF for rotational motion (method I).

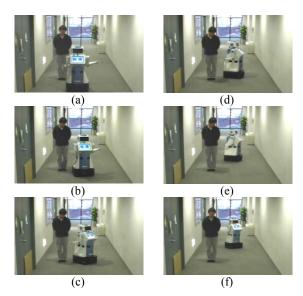

(a)   (d)

(b)   (e)

(c)   (f)

Figure 25: Experimental result to static human using fuzzy potential method with PMF for rotational motion (method II).
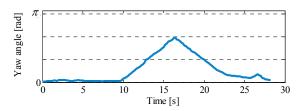
Figure 26: Time history of yaw angle of the robot.

The upper limit of the velocity of the robot was 0.5 m/s. The upper limit of the acceleration of the robot was 1.0 m/s^2. The arm position was set as shown in Figure 22. Figures 23(a) and 24 showed that the robot with method I can reach the goal without colliding with the obstacle. However, the position of the right arm comes close to the right-side wall.

On the other hand, it was confirmed in Figures 23(b), 25 and 26 that the robot with the proposed method (method II) changes the orientation angle of the robot to keep the safe distance with the right-side wall and can reach the goal point without colliding with the obstacle.

5 CONCLUSIONS

In this paper, the real-time collision avoidance method with simultaneous control of both translational and rotational motion with consideration of a robot width for an autonomous mobile robot, which is horizontally long, has been proposed. This method used an omni-directional platform for the drive system and was based on the fuzzy potential method. The novel design method of potential membership function, which takes the robot's size into consideration using the capsule case, was introduced. With the proposed method, the wide robot can decide the direction of translational motion to avoid obstacles safely. In addition, by controlling rotational motion in real time, the wide robot moves while keeping a safe distance with surroundings in narrow space. The effectiveness has been verified by numerical simulations and experiments. It has been shown that the proposed method performs translational and rotational motion simultaneously according to the situation.

REFERENCES

Kavraki, L., 1995. Computation of Configuration Space Obstacles Using the Fast Fourier Transform, *IEEE Trans. on Robotics and Automation*, Vol. 11, No. 3, pp. 408-413.

Wang, Y., Chirikjian, G. S., 2000. A New Potential Field Method for Robot Path Planning, *Proc. IEEE Int. Conf. on Robotics and Automation*, San Francisco, CA, pp. 977-982.

Ambrose, R. O., Savely, R. T., Goza, S. M., Strawser, P., Diftler, M. A., Spain, I., and Radford, N., 2004. Mobile manipulation using NASA's robonaut, *Proc. IEEE ICRA*, pp. 2104-2109.

Du, Z., Qu, D., Yu, F. and Xu, D, 2007. A Hybrid Approach for Mobile Robot Path Planning in Dynamic Environments, *Proc. IEEE Int. Conf. on Robotics and Biomimetics*, pp.1058-1063.

Khatib, O., 1986. Real-time Obstacle Avoidance for Manipulators and Mobile Robots, *Int. J. of Robotics Research*, Vol.5, No.1, pp.90-98.

Koren, Y., and Borenstein, J., 1991. Potential Field Methods and Their Inherent Limitations for Mobile Robot Navigation, *Proc. IEEE Int. Conf. on Robotics and Automation*, pp.1398-1404.

Borenstein, J., Koren, Y. , 1989. Real-Time Obstacle Avoidance for Fast Mobile Robots, *IEEE Trans. on Systems, Man, and Cybernetics*, Vol.19, No.5, pp.1179-1187.

Borenstein, J., Koren, Y., 1991. The Vector Field Histogram Fast Obstacle Avoidance for Mobile Robots, *IEEE Trans. on Robotics and Automation*, Vol.7, No.3, pp.278-288.

Lumelsky, V. J., Cheung, E. , 1993. Real Time Obstacle Collistion Avoidance in Teleoperated Whole Sensitive Robot Arm Manipulators, *IEEE Trans. Systems, Man, and Cybernetics*, Vol.23, No.1, pp.194-203.

Borenstein, J., Koren, Y., 1991. The Vector Field Histogram Fast Obstacle Avoidance for Mobile Robots, *IEEE Trans. on Robotics and Automation*, Vol.7, No.3, pp.278-288.

Dieter, F., Wolfram, B., Sebastian, T., 1997. The Dynamic Window Approach to Collision Avoidance, *IEEE Robotics and Automation*, Vol. 4, No. 1, pp.1-23.

Tsuzaki, R., Yoshida, K., 2003. Motion Control Based on Fuzzy Potential Method for Autonomous Mobile Robot with Omnidirectional Vision". *Journal of the Robotics Society of Japan*, Vol.21, No.6, pp.656-662.

Takahashi, M., Suzuki, T., 2009. Multi Scale Moving Control Method for Autonomous Omni-directional Mobile Robot, *Proc. of the 6th Int. Conf. on Informatics in Control, Automation and Robotics*.